IIETA International Information and Engineering Technology Association
Advancing the World of Information and Engineering

Journal Européen des Systèmes Automatisés
Vol. 56, No. 2, April, 2023, pp. 345-353
Journal homepage: http://iieta.org/journals/jesa

Optimal Fractional Order Proportional Integral Controller for Dual Star Induction Motor Based on Particle Swarm Optimization Algorithm

Es-saadi Terfia[1*], Salah Eddine Rezgui[2], Sofiane Mendaci[3], Hamza Gasmi[4], Hocine Benalla[2]

[1] Laboratory of Electrical Engineering of Guelma (LGEG), Department of Electrical Engineering and Automatic, Université 8 Mai 1945, Guelma 24000, Algeria
[2] Laboratory of Electrotechnics of Constantine, Department of Electrical Engineering, Engineer Sciences Faculty, Frères Mentouri Constantine 1 University, Constantine 25000, Algeria
[3] Laboratoire d'Automatique et Informatique de Guelma (LAIG), Department of Electrical Engineering and Automatic, Université 8 Mai 1945, Guelma 24000, Algeria
[4] Laboratoire de Contrôle Avancé (LABCAV), Department of Electronic and Telecommunication, Université 8 Mai 1945, Guelma 24000, Algeria

Corresponding Author Email: terfia.es-saadi@univ-guelma.dz

https://doi.org/10.18280/jesa.560220

Received: 6 February 2023
Accepted: 13 April 2023

Keywords:
DTC, DSIM, Control, FOPI, PSO

ABSTRACT

The purpose of this paper is to improve the performance of the conventional direct torque control (DTC) method of a dual star induction motor (DSIM) by enhancing speed control and reducing the ripples of electromagnetic torque and stator current. To achieve this, we propose a new optimal tuned controller based on the combination of a fractional order proportional integral controller (FOPI) and particle swarm optimization (PSO) algorithm. The aim of this high-performance controller is to reduce the rise time, settling time, steady-state error, and effects of load disturbances in the speed response of the DSIM, as well as minimize oscillations in the torque and stator currents, particularly at low speeds. This strategy named DTC-FOPI-PSO will be investigated, and its performances will be compared with the traditional DTC strategy based on the classical PI controller. Simulation tests using MATLAB/Simulink software are conducted under different operating conditions to demonstrate that the proposed DTC-FOPI-PSO strategy has a direct impact on improving speed dynamic, reducing torque fluctuations, minimizing steady-state error and provides excellent performance for load variation and reference speed inversion.

1. INTRODUCTION

In high-power applications, AC machines powered by static converters occupy increasingly industrial areas. However, the constraints on the power components limit the switching frequency and, thus, the performance. Therefore, the power must be segmented to enable the use of components with higher switching frequencies [1-3]. One way to ensure this is to use large phase (or multi-phase) machines, and as an example of this type is the dual star induction motor.

Dual star induction motor has noticeable potential because of their reliability and ability to operate in degraded conditions [4, 5]. However, despite these advantages, their control remains rather complicated compared to the DC machines because the mathematical model is non-linear and intrinsically coupled [6, 7].

To guaranty good performance and decoupling control, one can use direct torque control. This is a vector control method introduced by TAKAHASHI and DEPENBROCK. It's considered as an alternative approach because of its efficiency and simplicity of implementation [8].

This technique is based on the calculation of the stator flux and the electromagnetic torque from stator currents and voltages measurements without the need of a speed sensor [9]. It has been proven that the DTC has remarkable dynamic performance and is recognized as a reliable and robust solution to meet high control requirements [10-12].

Improving system performances is the main objective of the control techniques. For this purpose, different techniques are used, including linear and non-linear approaches. The simpler and effective solutions that exist nowadays in the majority of engineering control applications employ proportional integral derivative (PID) in the regulation loop [13]. On the other hand, lots of nonlinear control laws have been proposed including sliding mode control (SMC) [14, 15], synergetic control [16-18], predictive control [19], backstepping control [20, 21], and high-order SMC techniques [5]. In addition, the response and the speed dynamic of a system can be improved using intelligent techniques, such as fuzzy logic and neural networks [22-24].

However, PID controllers are limited and cannot meet all the needs of a variable speed drives.

There is strong evidence that PI and PI tuned by PSO controllers continue to be poorly understood and, in particular, inadequately tuned in many applications during the last few years [25].

Numerous strategies have been suggested to deal with these problems. One recommendation is to reinforce the proportional-integral-derivative controller's flexibility, robustness, and stability by introducing two additional fractional non-integer differentiation and integration control parameters and then get a fractional-order controller. Some

recent researches recommended fractional order (FOPID) control for robust control [26, 27].

In this context, with the aim of improving the features of the traditional DTC, we propose an approach based on FOPI controller and the particle swarm optimization technique, named FOPI-PSO.

The fact that the FOPI controller contains an additional parameter, will makes the FOPI-PSO more flexible than the classic PI controller. Moreover, the performance of the DSIM system will be enhanced as a result of the designed FOPI-PSO method.

The strategy of this work is to tune the parameters of the FOPI controller using the PSO algorithm in order to achieve accurate tuning that corresponds to the high performance required in DTC control of the DSIM. This includes minimizing the rise time, settling time, steady-state error, impact of disturbances on speed control, as well as reducing torque and stator current ripples.

The study is organized as follows: Section 1 presents the DSIM mathematical model; Section 2 presents the conventional DTC control of the dual star induction motor. Sections 3 and 4 introduce the concept of a fractional order PID controller and the PSO optimization method, respectively. Section 5 includes a detailed description of the proposed strategy with the DTC using the PSO algorithm. The results, discussions, and conclusion complete the study.

2. DSIM MATHEMATICAL MODEL

The stator of the DSIM consists of two three-phase systems (a_{s1}, b_{s1}, c_{s1}) and (a_{s2}, b_{s2}, c_{s2}), separated by an electrical angle α of 30 degrees, as shown in Figure 1. The rotor consists of a classic three-phase system (a_r, b_r, c_r), which is identical to that of the induction motor.

By using Park's method, the three-phase scheme of the DSIM (specified in Figure 1) is transformed into a two-phase model (d-q). Hence, the stator and rotor voltages elements are expressed in d-q frame as follows [28]:

$$\begin{cases} V_{s1d} = R_{s1}I_{s1d} + \dfrac{d\Phi_{s1d}}{dt} - \omega_s\Phi_{s1q} \\ V_{s1q} = R_{s1}I_{s1q} + \dfrac{d\Phi_{s1q}}{dt} + \omega_s\Phi_{s1d} \\ V_{s2d} = R_{s2}I_{s2d} + \dfrac{d\Phi_{s2d}}{dt} - \omega_s\Phi_{s2q} \\ V_{s2q} = R_{s2}I_{s2q} + \dfrac{d\Phi_{s2q}}{dt} + \omega_s\Phi_{s2d} \\ V_{rd} = 0 = R_rI_{rd} + \dfrac{d\Phi_{rd}}{dt} - \omega_{sr}\Phi_{rq} \\ V_{rq} = 0 = R_rI_{rq} + \dfrac{d\Phi_{rq}}{dt} + \omega_{sr}\Phi_{rd} \end{cases} \quad (1)$$

where,

V_{s1d}, V_{s1q}, V_{s2d} and V_{s2q} are the d-q voltage components of the two stator three-phase systems.

I_{s1d}, I_{s1q}, I_{s2d} and I_{s2q} are the d-q stator current components of the two stator systems.

I_{rd} and I_{rq} are the d-q current components of the rotor.

R_{s1} and R_{s2} are the stator resistances.

R_r is the rotor resistance.

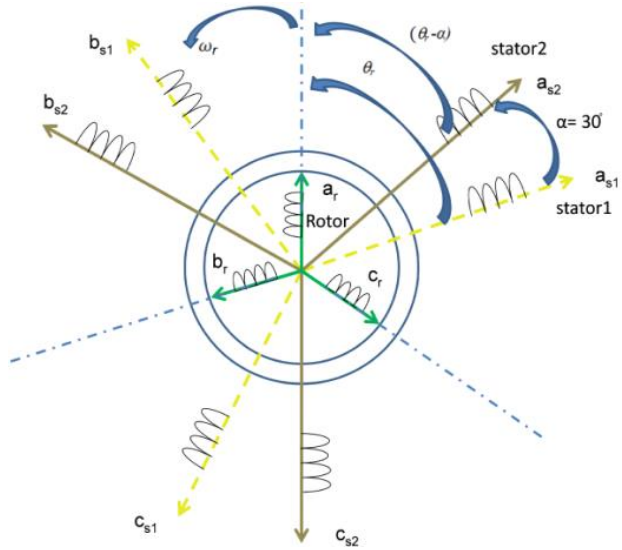

Figure 1. Representation of the DSIM winding

The stator and rotor flux components Φ_{s1d}, Φ_{s1q}, Φ_{s2d}, Φ_{s2q}, Φ_{rd} and Φ_{rq} are given by:

$$\begin{cases} \Phi_{s1d} = L_{s1}I_{s1d} + L_m\left(I_{s1d} + I_{s2d} + I_{rd}\right) \\ \Phi_{s1q} = L_{s1}I_{s1q} + L_m\left(I_{s1q} + I_{s2q} + I_{rq}\right) \\ \Phi_{s2d} = L_{s2}I_{s2d} + L_m\left(I_{s2d} + I_{s2d} + I_{rd}\right) \\ \Phi_{s2q} = L_{s2}I_{s2q} + L_m\left(I_{s1q} + I_{s2q} + I_{rq}\right) \\ \Phi_{rd} = L_rI_{rd} + L_m\left(I_{s1d} + I_{s2d} + I_{rd}\right) \\ \Phi_{rq} = L_rI_{rq} + L_m\left(I_{s1q} + I_{s2q} + I_{rq}\right) \end{cases} \quad (2)$$

where,

L_{s1} and L_{s2} are the stator inductances.

L_r is the rotor inductance.

L_m is the mutual inductance.

The mechanical speed formulation is given by:

$$J\frac{d\Omega}{dt} = T_{em} - T_L - F_r\Omega \quad (3)$$

where, the relation of the electromagnetic torque T_{em} is as below:

$$T_{em} = p\frac{L_m}{L_r + L_m}\left[\Phi_{rd}\left(I_{s1q} + I_{s2q}\right) - \Phi_{rq}\left(I_{s1d} + I_{s2d}\right)\right] \quad (4)$$

where,

p denotes the number of pole pairs.

J represents the total moment of inertia.

F_r is the viscous friction coefficient.

T_L denotes the load torque.

3. TRADITIONAL DTC OF DSIM

The DTC was proposed by Takahashi and Noguchi [8] in the mid-1980s. The principle of this control is to directly control the torque and the stator flux of the machine. In this context, the hysteresis comparators are used which allow comparing the estimated values with those of references, then the inverter states are directly controlled through a predefined selection table. Compared to field-oriented control, DTC is less sensitive to parametric variations of the machine and allows obtaining precise and fast torque dynamics. The DTC control strategy of the DSIM is illustrated in Figure 2. The main components of its structure with a speed loop regulator are defined as follows:

- Estimators for torque and stator flux based on the stator-related model.
- A selection table, of the desired stator voltage vector, established in accordance with the generated flux and torque. The classical selection table is given in Table 1, where C_{flx} and C_{cpl} are the status of the flux and torque error respectively.
- Hysteresis comparators, one with two levels for flux control, the other one with three levels dedicated to the control of the electromagnetic torque.
- A speed regulator.

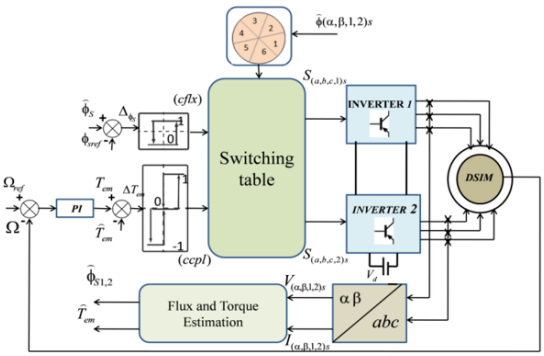

Figure 2. The classical DTC control structure of DSIM using a PI controller for the speed loop

Table 1. Switching table of the classical DTC control strategy

Sector		1	2	3	4	5	6	Comparator
C_{flx}=1	C_{cpl}=1	V_2	V_3	V_4	V_5	V_6	V_1	2 levels
	C_{cpl}=0	V_7	V_0	V_7	V_0	V_7	V_0	
	C_{cpl}=-1	V_6	V_1	V_2	V_3	V_4	V_5	3 levels
C_{flx}=0	C_{cpl}=1	V_3	V_4	V_5	V_6	V_1	V_2	2 levels
	C_{cpl}=0	V_0	V_7	V_0	V_7	V_0	V_7	
	C_{cpl}=-1	V_5	V_6	V_1	V_2	V_3	V_4	3 levels

The following equations give the expression for the stator flux estimation:

$$\begin{cases} \Phi_{s\alpha 1,2} = \int_0^t \left(V_{s\alpha 1,2} - R_s i_{s\alpha 1,2}\right) dt \\ \Phi_{s\beta 1,2} = \int_0^t \left(V_{s\beta 1,2} - R_s i_{s\beta 1,2}\right) dt \end{cases} \quad (5)$$

where, $V_{s\alpha 1,2}$ and $V_{s\beta 1,2}$ are the stator vector voltage components in the α-β fixed frame. They are measured or obtained using the inverter model.

4. FOPID CONTROLLER CONCEPT

Fractional order PID controller indicated by FOPID was suggested by Podlubny et al. [29] in 1997.

The FOPID is an extension of the PID controller, vastly used in the industrial control system. The FOPID is based on fractional calculus. FOPID has five parameters which are accountable for providing good behavior of dynamical systems and low sensitivity to parameters changing in a controlled system [30].

The integer-differential Equation (6) gives the control law of the fractional order PID controller [31].

$$u(t) = K_p e(t) + K_i D^{-\lambda} e(t) + K_d D^{\mu} e(t) \quad (6)$$

The input signal $e(t)$, the command signal $u(t)$, the proportional gain K_p, the integration gain K_i, and the derivative gain K_d are all represented in Equation 6. The integral and derivative terms that are not integer orders are named λ and μ, respectively.

An operator for fractional derivatives and integrals is called D^{α}. The most commonly used definition of the fractional operator, known as the Riemann-Liouville description, is as follows [32, 33]:

$${}_a D_t^{\alpha} f(t) = \frac{1}{\Gamma(n-\alpha)} \frac{d^n}{dt^n} \left[\int_a^t \frac{f(\tau)}{(t-\tau)^{\alpha-n+1}} d\tau \right] \quad (7)$$

The gamma expression of Euler is represented by $\Gamma(.)$, the integration limits are a and t, and n is an integer that fits the condition $n\text{-}1 < \alpha < n$.

The following equation provides the Laplace transform of Equation (6) for zero initial conditions:

$$L\left\{ {}_a D_t^{\alpha} f(t) \right\} = \int_0^{\infty} e^{-st} {}_a D_t^{\alpha} f(t) dt = s^{\alpha} F(s) \quad (8)$$

Then, the transfer function of the FOPID controller is given by Equation (9) as follows:

$$G(s) = K_p + K_i s^{-\lambda} + K_d s^{\mu} \quad (9)$$

Obviously, taking $\lambda = 1$ and $\mu = 1$, one can obtain a classic PID.

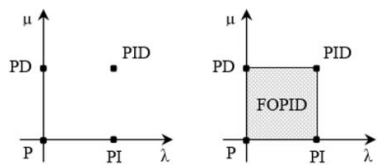

Figure 3. Classical PID controller versus FOPID controller

The FOPID controller expands the traditional PID controller from a point to a plane, as depicted in Figure 3. The flexibility and robustness of this generalized controller allows

us to more precisely manage the dynamics of the control system, and as a result, the system becomes robust and more stable [31].

The structure of a FOPI ($K_d = 0$) is selected, which is the PI controller's general form.

5. THE PSO OPTIMIZATION ALGORITHM

The particle swarm optimization algorithm is one of the most widely used methods today for solving optimization problems. Due to its low computational cost, high performance, and simplicity, it has been hailed as a potential and successful optimization technique. PSO algorithms are used in many scientific fields, which successfully solve most optimization problems [34, 35].

Midway through the 1990s, Kennedy and Eberhart [36] created the PSO algorithm as a heuristic search technique. The social behavior and movement of a collection of birds or a group of fish looking for food is the basis for PSO. Particles (possible solutions) fly across the search space, looking for attractive locations based on previous experiences and those of their neighbors, according to how the PSO algorithm operates [37, 38]. The PSO technique is recommended in this study to tune the controller gains to achieve the optimal controller parameters and, as a result, the best system output.

At each cycle, the following calculations are made to determine each population particle's new velocity and position:

$$\begin{cases} v_i^{k+1} = wv_i^k + c_1 r_1 \left(Pbest_i^k - X_i^k \right) + c_2 r_2 \left(Gbest_i^k - X_i^k \right) \\ r_1, r_2 \in [0,1] \text{ are random numbers} \end{cases} \quad (10)$$

$$X_i^{k+1} = X_i^k + v_i^{k+1} \quad (11)$$

where, $Gbest_i^k$ is the global best solution and $Pbest_i^k$ is the personal best solution.

Equation (12) represents the integral of absolute error (IAE) between the speed Ω and its reference Ω_{ref}. The IAE is used to build the objective function that will be optimized,

$$IAE = \int_0^\infty \left(|\Delta\Omega| \right) dt \quad (12)$$

where,

$$\Delta\Omega = \Omega_{ref} - \Omega \quad (13)$$

To optimize the parameters of the FOPI controller offline, it is recommended to vary the speed and load in different scenarios during the execution of the PSO algorithm. This optimization approach can improve speed dynamics, reduce torque oscillations, and minimize steady-state errors.

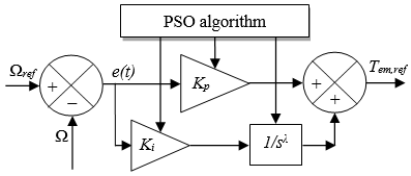

Figure 4. Proposed FOPI-PSO controller concept

The proposed FOPI-PSO controller is illustrated in Figure 4, it contains three parameters (K_p, K_i and λ) to be optimized offline by the PSO method. This optimized controller will provide at its output the reference torque necessary to control the speed with precision and more robustness than the conventional PI controller.

6. PROPOSED DTC OF DSIM WITH FOPI-PSO

The PSO method is used to implement the optimization steps of the FOPI controller for controlling the DSIM speed. Figure 5 depicts these actions in the order they should be taken.

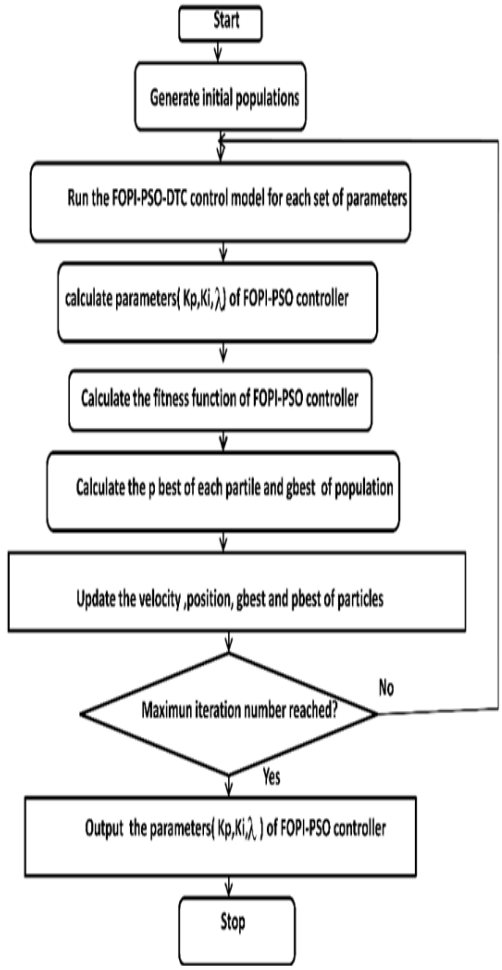

Figure 5. Flowchart of FOPI-PSO-DTC-DSIM

Table 2 provides a list of the control parameters for the PSO method used to optimize the FOPI controller.

Table 2. Parameters of the PSO algorithm

Parameter	Value
Swarm size	50
Maximum iteration	100
c_1	0.1
c_2	1.2
w	0.8

The proposed DTC method with the DSIM's FOPI-PSO algorithm is shown in Figure 6.

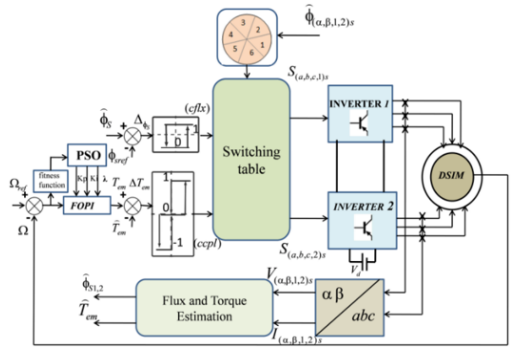

Figure 6. Schematic of DTC of DSIM with FOPI-PSO

7. SIMULATION RESULTS AND DISCUSSION

To validate the performance of the proposed approach and compare it with to the classical technique, a simulation was carried out in MATLAB/Simulink software, the control diagram depicted in Figure 6 is implemented using the parameters that are presented in Table 3.

Two control techniques which are: classical PI and the proposed one (FOPI-PSO) are tested in two scenarios.

Table 3. Specifications parameters of DSIM [39]

Parameter	Value
Rated power	4.5 kW
Stator resistance ($R_{s1} = R_{s2}$)	3.72 Ω
Rotor resistance (R_r)	2.12 Ω
Stator self-inductance ($L_{s1} = L_{s2}$)	0.022 H
Rotor self-inductance (L_r)	0.006 H
Cyclic mutual inductance (L_m)	0.3672H
Pole pair number (P)	1
Moment of inertia (J)	0.0662 kg.m^2
Friction coefficient (F_r)	0.001N.m.s/rad

7.1 Tracking test

The first scenario is when the DSIM is started with a reference command until the speed reaches the set point (100 rad/s) under no load. The second scenario aims to test the dynamic response after the application of a load step.

Figure 7 shows that the speed follows its references perfectly for the two controllers, PI and FOPI-PSO. However, better speed control precision is obtained with the proposed FOPI-PSO strategy. It is observed that the FOPI-PSO has superior performances in terms of the rise time and settling time, where the rise time is 0.1751 s and 0.1908 s for FOPI-PSO and PI respectively, and the settling times are 0.1941s and 0.2123s.

After introducing the load (14 N.m) at t=0.7s, the proposed FOPI-PSO method shows a fast disturbance rejection in a very short time with no steady-state error. On the other hand, we can observe that the classical PI controller is suffering from a speed drop and a permanent steady-state error.

Figure 8 illustrates the torque dynamic performance. It is visible that the torque ripples obtained by the proposed FOPI-PSO controller are lower than those obtained by the traditional techniques based on the PI controller. The use of FOPI-PSO controller contributes in mitigating fluctuations and refining the stator currents wave form.

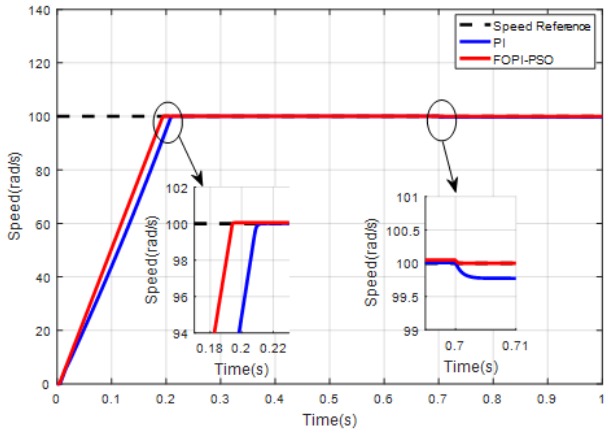

Figure 7. Speed response of the DSIM

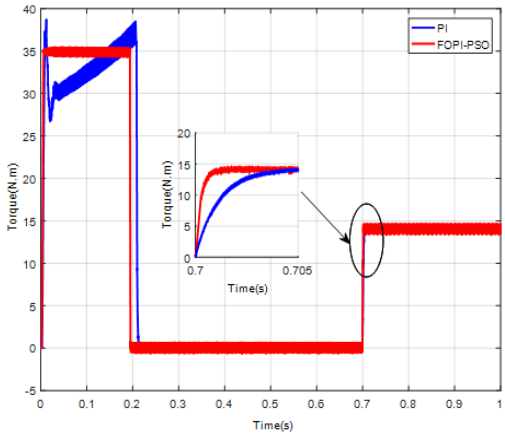

Figure 8. The electromagnetic torque response

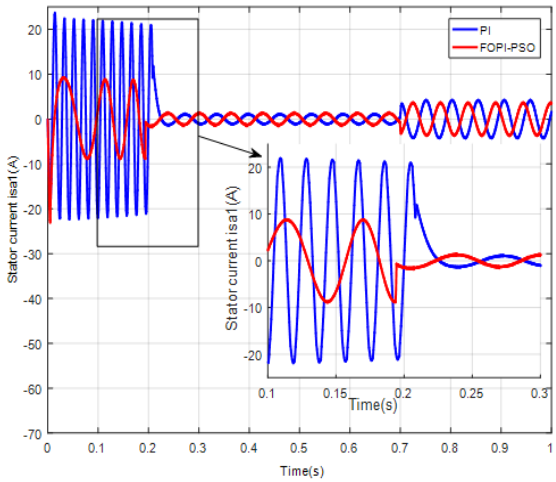

Figure 9. Stator current in winding (1)

Figure 9 shows the phase stator current (I_{sa1}). It has a sinusoidal shape and less current ripples in the case of the proposed FOPI-PSO controller compared to the PI controller which has a large current ripple. To obtain a good system output response, the FOPI-PSO controller has good results and well-tuned values. As a result of this action, the performance constraints, including rise time, settling time, steady-state error and disturbance rejection, are reduced considerably. Table 4 shows the results obtained for the different controllers. The high reduction ratios, with percentages of 8.22% and 8.57% for each of the rise time and the settling time respectively, indicates that the proposed FOPI-PSO controller is more

effective in improving the rise time, settling time and steady state error than the classical PI controller.

Table 4. Comparison between PI and FOPI-PSO

Criteria	PI	FOPI-PSO
Rise time (sec)	0.1908	0.1751
Settling time (sec)	0.2123	0.1941
Dynamic response(sec)	Medium	Very fast
Speed tracking	Good	Excellent
Steady state error (%)	>3	Negligible
Torque ripples reduction	Medium	Very well
Minimizing the stator current ripples	Medium	Very well
Stator current quality	Acceptable	Excellent

Table 4 lists a comparison between performances of the proposed method and the classical PI technique. The proposed FOPI-PSO improved all the performance criteria, compared to the PI controller.

7.2 Robustness test

Concerning the speed changing and load variation, this test examines the effectiveness and validity of the proposed method. The following conditions are applied to the system during simulation:

- At first, the reference speed is fixed at 100 rad/s, and it is changed at t=1s from 100 to 50 rad/s, and switched from 50 to -50 rad/s at t=2s, and finally set to -100 rad/s at t=3s.
- The motor starts with no load until t=0.7 s, we introduce a load torque of 14 N.m, and after the load becomes 10 N.m at t=1.6 s.
- The flux amplitude is kept constant at 1 Wb.

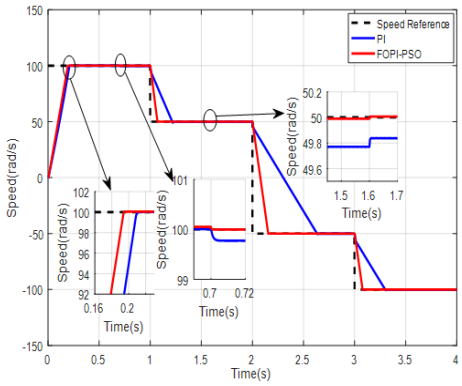

Figure 10. Speed tracking of the DSIM

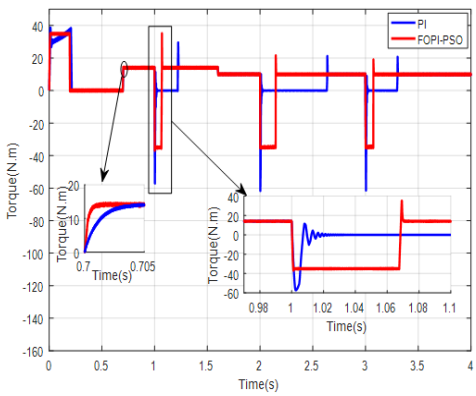

Figure 11. Electromagnetic torque

Figures 10-12 exhibit the results of the test, where we can observe the curves of the stator current (I_{sa1}), the speed, and the electromagnetic torque.

Figure 10 illustrates the variation of the rotor speed. For both methods PI and FOPI-PSO, it can be seen that the speed absolutely complies with their references when we apply a various amount of the load.

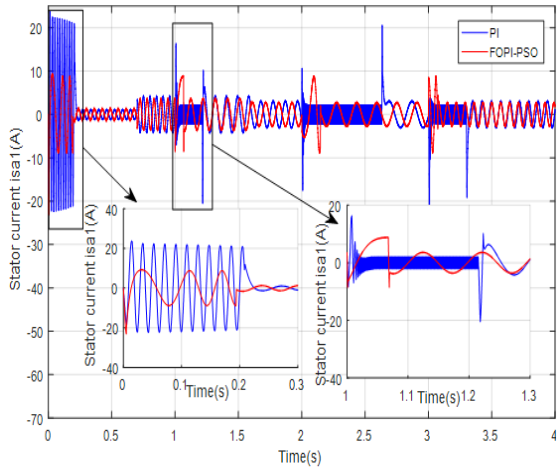

Figure 12. Stator current in winding (1)

However, the proposed FOPI-PSO technique yields greater speed control accuracy, and performs better than classical method in terms of rise time, settling time, steady-state error and disturbance rejection.

The dynamic response of the torque is shown in Figure 11. It is clear that the suggested FOPI-PSO controller produces lower torque ripples than those produced by conventional PI method under speed and load variation.

The phase stator current (I_{sa1}) is depicted in Figure 12. Using FOPI-PSO controller leads to a sinusoidal current shape with fewer ripples compared to the conventional PI controller, which exhibits significant current ripple when the speed and load torque are varied.

8. CONCLUSION

In this research paper, we have presented a DTC-FOPI-PSO method to enhance the system performance of the control of a DSIM.

Because it includes more parameters compared to the classic PI regulator, the proposed FOPI-PSO controller has been proved more adaptable and efficient, despite that, tuning several parameters was a challenging task. For that, the PSO optimization method was employed to determine the optimal parameters of the FOPI controllers.

According to simulation results, the proposed DTC-FOPI-PSO method showed superior behavior in different tests when compared to classical methods and other existing works.

The benefits of the proposed DTC-FOPI-PSO can be summarized in the following points:

- Compared to the traditional DTC technique based on the PI controller, the rise time, settling time, steady-state error and disturbance effects are decreased.
- Significant reduction in the ripples of the electromagnetic torque and stator currents.

For future research, we recommend exploring the following suggestions:

- Combining the FOPI fractional controller with a sliding mode controller to increase robustness to disturbances.
- Using multi-objective optimization techniques to optimize several criteria simultaneously, resulting in multiple Pareto-optimal solutions that can be selected according to the desired specifications.
- Applying the proposed controller to other types of motors and systems.

REFERENCES

[1] Hadiouche, D., Razik, H.,Rezzoug, A. (2004). On the modeling and design of dual-stator windings to minimize circulating harmonic currents for VSI fed AC machines. IEEE Transactions on Industry Applications, 40(2): 506-515. https://doi.org/10.1109/TIA.2004.824511

[2] Moati, Y., Kouzi, K. (2020). Investigating the performances of direct torque and flux control for dual stator induction motor with direct and indirect matrix converter. PeriodicaPolytechnica Electrical Engineering and Computer Science, 64(1): 97-105. https://doi.org/10.3311/PPee.14977

[3] Oumar, A., Ahmed, Y., Cherkaoui, M. (2022). Operating of DSIM without current and speed sensors controlled by ADRC control. Mathematical Problems in Engineering, 2022: 9033780. https://doi.org/10.1155/2022/9033780

[4] Hadiouche, D., Baghli, L., and Rezzoug, A. (2006). Space-vector PWM techniques for dual three-phase AC machine: Analysis, performance evaluation, and DSP implementation. IEEE Transactions on Industry Applications, 42(4): 1112-1122. https://doi.org/10.1109/TIA.2006.877737

[5] Boukhalfa, G., Belkacem, S., Chikhi, A., Bouhentala, M. (2022). Fuzzy-second order sliding mode control optimized by genetic algorithm applied in direct torque control of dual star induction motor. Journal of Central South University, 29(12): 3974-3985. https://doi.org/10.1007/s11771-022-5028-3

[6] Moati, Y., Kouzi, K. (2020). An efficient of direct torque control of indirect three level matrix converter fed dual stator induction motor based on synergetic controller. Journal Européen des Systèmes Automatisés, 53(5): 617-627. https://doi.org/10.18280/jesa.530504

[7] Adjati, A., Rekioua, T., Rekioua, D. and Tounzi, A. (2020). Study of dual stator induction motor in photovoltaic-fuel cell hybrid pumping application. Journal Européen des Systèmes Automatisés, 53(5): 601-608. https://doi.org/10.18280/jesa.530502

[8] Takahashi, I., Noguchi, T. (1986). A new quick-response and high-efficiency control strategy of an induction motor. IEEE Transactions on Industry Applications, IA-22(5): 820-827. https://doi.org/10.1109/TIA.1986.4504799

[9] Benyoussef, E., Said, B. (2022). Five-Level DTC-ANN with balancing strategy of DSIM. International Journal of Energy, 16(22): 52-59. https://doi.org/10.46300/91010.2022.16.8

[10] Lazreg, M., Bentaallah, A. (2019). Sensorless Speed Control of Double Star Induction Machine with Five Level DTC Exploiting Neural Network and Extended Kalman Filter, Iranian Journal of Electrical and Electronic Engineering, 15(1): 142-150. https://doi.org/10.22068/IJEEE.15.1.142

[11] Tatte, Y., Aware, M., Badoni, M (2022). Modified direct torque control technique of induction motor for torque ripple and common-mode voltage reduction with neutral-point voltage balancing.Iranian Journal of Science and Technology, Transactions of Electrical Engineering, 46: 1207-1221. https://doi.org/10.1007/s40998-022-00533-1

[12] Boukhalfa, G., Belkacem, S., Chikhi, A. and Benaggoune, S. (2022). Direct torque control of dual star induction motor using a fuzzy-PSO hybrid approach, Applied Computing and Informatics, 18(1/2): 74-89. https://doi.org/10.1016/j.aci.2018.09.001

[13] Boukhalfa, G., Belkacem, S., Chikhi, A., Benaggoune, S. (2019). Genetic algorithm and particle swarm optimization tuned fuzzy PID controller on direct torque control of dual star induction motor. Journal of Central South University, 26(7): 1886-1896.https://doi.org/10.1007/s11771-019-4142-3

[14] Beghdadi, A., Bentaallah, A. Abden, A. (2021). Optimization of sliding mode with MRAS based estimation for speed sensorless control of DSIM Via GWO. Przegląd Elektrotechniczny, 97(6): 21-29. https://doi.org/10.15199/48.2021.06.04

[15] Layadi, N., Djerioui, A., Zeghlache, S., Mekki, H., Houari, A., Gong, J., Berrabah, F. (2020). Fault-tolerant control based on sliding mode controller for double-star induction machine. Arabian Journal for Science and Engineering, 45(3): 1615-1627. https://doi.org/10.1007/s13369-019-04120-1

[16] Guermit, H., Kouzi, K., Bessedik, S.A. (2019). Novel Design of an Optimized Synergetic Control for Dual Stator Induction Motor. COMPEL-The International Journal for Computation and Mathematics in Electrical and Electronic Engineering, 38(6): 1828-1845. https://doi.org/10.1108/COMPEL-01-2019-0042

[17] Belouahchi, F., Merabet, E. (2020). Design of a new direct torque control using synergetic theory for double star induction motor. Journal Européen des Systèmes Automatisés, 53(6): 903-914. https://doi.org/10.18280/jesa.530616

[18] Moati, Y., Kouzi, K., and Iqbal, A. (2021). Adaptive optimized DTC-SVM using metaheuristic bat algorithm for DSIM fed by IMC based on robust synergetic speed controller. International Transactions on Electrical Energy Systems, 31(1): e12697. https://doi.org/10.1002/2050-7038.12697

[19] Khouidmi, H., Massoum, A. (2019). Predictive control based speed, torque and flux prediction of a double stator induction motor. Majlesi Journal of Electrical Engineering,13(1): 65-77.

[20] Rahali, H., Zeghlache, S., Benyettou, L., Benalia, L. (2019). Backstepping sliding mode controller improved with interval type-2 fuzzy logic applied to the dual star induction motor. International Journal of Computational Intelligence and Applications, 18(2): 1950012. https://doi.org/10.1142/S1469026819500123

[21] Chaabane, H., Eddine, K. D., and Salim, C. (2020).Sensorless backstepping control using a Lemberger observer for double-star induction motor. Archives of Electrical Engineering, 69(1): 101-116. https://doi.org/10.24425/aee.2020.131761

[22] Meroufel, A., Massoum, S., Bentaallah, A., Wira, P., Belaimeche, F.Z., Massoum, A. (2017). Double star induction motor direct torque control with fuzzy sliding mode speed controller.Revue Roumaine des Sciences Techniques. Serie Électrotechnique et Énergétique, 1: 31-35.

[23] Himour, K., Yahiaoui, A. Iffouzar, K. (2020). Comparison of different control strategies of multilevel inverters used to fed a dual star induction machine. Journal Européen des Systèmes Automatisés, 53(4): 525-532. https://doi.org/10.18280/jesa.530411

[24] Hellali, L., Belhamdi, S., Loutfi, B., Hassen, R. (2018). Direct torque control of doubly star induction machine fed by voltage source inverter using type-2 fuzzy logic speed controller. Advances in Modelling and Analysis C, 73(4): 202-207. https://doi.org/10.18280/ama_c.730410

[25] Meliani, B., Meroufel, A. (2017). PSO based tuning of pi controller for a dual star induction machine fed by a five-level inverter.International Journal of Electrical Engineering & Technology, 8(4): 26-35.

[26] Gasmi, H., Mendaci, S., Laifa, S., Kantas, W., Benbouhenni, H. (2022). Fractional-order proportional-integral super twisting sliding mode controller for wind energy conversion system equipped with doubly fed induction generator. Journal of Power Electronics, 22: 1357-1373. https://doi.org/10.1007/s43236-022-00430-0

[27] Warrier, P., Shah, P. (2021). Fractional order control of power electronic converters in industrial drives and renewable energy systems: A review. IEEE Access, 9: 58982-59009. https://doi.org/10.1109/ACCESS. 2021.3073033

[28] Che, H.S., Levi, E., Jones, M., Duran, M.J., Hew, W.P., Rahim, N.A. (2013). Operation of a six-phase induction machine using series-connected machine-side converters. IEEE Transactions on industrial Electronics, 61(1): 164-176. https://doi.org/10.1109/TIE.2013.2248338

[29] Podlubny, I., Dorcak, L., Kostial, I. (1997). On Fractional derivatives, fractional-order dynamic systems and PI/SUP/SPLLAMBDA//D/SUP/SPL MU//-controllers. IEEE Transactions on Automatic Control, 44(5): 4985-4990. https://doi.org/10.1109/9.739144

[30] El-Dabah, M.A., Kamel, S., Abido, M.A.Y., Khan, B. (2022). Optimal tuning of fractional-order proportional, integral, derivative and tilt-integral-derivative based power system stabilizers using runge kutta optimizer. Engineering Reports, 4(6): 1-12. https://doi.org/10.1002/eng2.12492

[31] Hamouda, N., Babes, B., Hamouda, C., Kahla, S., Ellinger, T., Petzoldt, J. (2020). Optimal Tuning of Fractional Order Proportional-Integral-Derivative Controller for Wire Feeder System Using Ant Colony Optimization. Journal Européen des Systèmes Automatisés, 53(2): 157-166. https://doi.org/10.18280/jesa.530201

[32] Barakat, M. H., Salama, G. M., Donkol, A., Hamed, H.F. (2021). Optimal Design of Fraction-Order Proportional-Derivative Proportional-Integral Controller for LFC of Thermal-Thermal-Wind Turbines Considering Nonlinearities. Journal of Advanced Engineering Trends, 41(2): 275-283. https://doi.org/10.21608/JAET.2021.64407.1090

[33] Muresan, C.I., Birs, I.R., Ionescu, C.M., De Keyser, R. (2019). Tuning of fractional order proportional integral/proportional derivative controllers based on existence conditions. proceedings of the institution of mechanical engineers, Part I. Journal of Systems and Control Engineering, 233(4): 384-391. https://doi.org/10.1177/0959651818790809

[34] Dashtdar, M., Flah, A., El-Bayeh, C.Z., Tostado-Véliz, M., Al Durra, A., Abdel Aleem, S.H., Ali, Z.M. (2022). Frequency control of the islanded microgrid based on optimised model predictive control by PSO. IET Renewable Power Generation, 16(1): 2088-2100. https://doi.org/10.1049/rpg2.12492

[35] Rayala, S.S., Kumar, N.A. (2020). Particle swarm optimization for robot target tracking application. Materials Today: Proceedings, 33(7): 3600-3603. https://doi.org/10.1016/j.matpr.2020.05.660

[36] Kennedy, J., Eberhart, R. (1995). Particle swarm optimization. In Proceedings of ICNN'95 - International Conference on Neural Networks, 4: 1942-1948. https://doi.org/10.1109/ICNN.1995.488968

[37] Pozna, C., Precup, R.E., Horvath, E., Petriu, E.M. (2022). Hybrid particle filter-particle swarm optimization algorithm and application to fuzzy controlled servo systems. IEEE Transactions on Fuzzy Systems, 30(10): 4286-4297. https://doi.org/10.1109/TFUZZ.2022.3146986

[38] Gasmi, H., Sofiane, M., Benbouhenni, H., Bizon, N. (2023). Optimal operation of doubly-fed induction generator used in a grid-connected wind power system. Iranian Journal of Electrical and Electronic Engineering, 19(2): 2431. https://doi.org/10.22068/IJEEE.19.2.2431

[39] Oudjebour, Z., Berkouk, E., Mahmoudi, M. (2012). Stabilization by new control technique of the input dc voltages of five-level diode-clamped inverters. application to double star induction machine. In 2nd International Symposium on Environment Friendly Energies and Applications, Newcastle Upon Tyne, UK, pp. 541-544. https://doi.org/10.1109/EFEA.2012.6294034

NOMENCLATURE

s	Stator index
r	Rotor index
$V_{ds1}, V_{qs1}, V_{ds2}, V_{qs2}$	Voltages in the d-q axis for stator 1 and 2, respectively
$I_{ds1}, I_{qs1}, I_{ds2}, I_{qs2}$	Currents in the d-q axis for stator 1 and 2, respectively
I_{dr}, I_{qr}	Rotor currents d-q axis components
$\Phi_{ds1}, \Phi_{qs1},$	Stator flux vectorsd-q axis components
Φ_{dr}, Φ_{qr}	Rotor flux vectors d-q axis components
T_{em}	Electromagnetic torque
T_L	Load torque
Ω_r	Mechanical speed
Ω_{ref}	Mechanical speed reference
ω_r	Angular speed for rotor
ω_s	Angular speed for stator
P	Number of pole pairs
J	Moment of Inertia
F_r	Friction coefficient
R_{s1}, R_{s2}	Stator resistances
R_r	Rotor resistance

L_{s1}, L_{s2}	Stator self-inductances
L_m	Cyclic mutual inductance
L_r	Rotor self-inductances
w	Inertia weight factor
c_1, c_2	The acceleration constant